Electro-Osmosis Drainage Capacity of a New Type of EKG Electrode

Yang Shen[1] and Yande Li[2]
[1,2]*College of Civil and Transportation Engineering, Hohai University, Nanjing, China*
[1]*E-mail*: shenyang1998@163.com
[2]*E-mail*: meilimeijia@126.com

ABSTRACT: The electro-kinetic geo-synthetics (EKG) electrode is a kind of electrode which may avoid the electrode corrosion and provide an effective drainage channel during the electro-osmosis process. Comparing tests between a new type of EKG electrode and the iron electrode were carried out. The drainage amount, drainage velocity, current, potential distribution, water content and cracks were monitored. Results showed that the iron electrode eroded seriously while the EKG electrode kept intact. In addition, drainage capacity on the soil's top surface of the EKG electrode was better than that of the iron electrode. The potential drop on the electrode-soil interface of the EKG electrode was smaller than that of the iron electrode when the anode was arranged in the hexagonal pattern. The water content increased gradually from the anode to the cathode for the iron electrode, while it increased at first and then decreased from the anode to the cathode for the EKG electrode.

KEYWORDS: Electro-osmosis, EKG electrode, Iron electrode, Voltages, Hexagonal pattern.

1. INTRODUCTION

Owing to its high moisture content, high compressibility, low intensity and some other characteristics, the bearing capacity of reclaimed ground needs to be improved before the buildings are constructed. The electro-osmosis method is an effective method which could discharge water from soil in a relatively short time by applying the DC voltage between the electrodes. However, the corrosion of the metal electrode and high energy consumption during the process limited its application (Shang et al. 1997).

The development of the electro-kinetic geo-synthetics (EKG) electrode has provided a potential solution to above problems. Jones et al. (2004) from Newcastle University firstly put forward the concept of EKG and defined its ability of filtration, drainage, reinforcement and conduction. The EKG electrode could be produced by using the conductive polymer composite only. In addition, it can also be produced by adding conductive materials to the polymer composite. Furthermore, the material could be manufactured into 2D or 3D shape according to different purposes, such as plate or tube (Jones et al. 2011).

Several types of EKG materials had been tested by Chinese scholars since 2000 (Hu et al. 2005), and the most efficacious method was to incorporate the carbon black and graphite with polyethylene, and then manufactured them into plate shape, similar with ordinary plastic drainage board (Zhuang et al. 2012). Some researches on the electrode material have been carried out by Huahong Full Electro-osmosis Technologies Co., Ltd in recent years and a new type EKG electrode was produced. In this paper, three kinds of comparative experiments on different voltages in the hexagonal electrode arrangement pattern between this new type of EKG electrode and an iron electrode were carried out. The electrode corrosion and the development regularity of cracks between the anode and cathode were qualitatively observed. The variation of drainage rate, drainage amount, the variation of current, and the potential distribution were monitored. The distribution of water content after the tests was quantitatively monitored. Finally, the advantages and disadvantages of the EKG electrode were discussed, and the methods to improve the treatment efficiency were proposed.

2. MATERIAL AND METHODS

2.1 Materials and equipment

The soil sample was obtained from a vacuum preloading field in Hexi Area of Nanjing. It was dried, crushed and mixed with water and finally made into remolded clay with 50% of water content before the test. The basic physical and mechanical properties of the soft clay are shown in Table 1.

Table 1 Physical and mechanical properties of the soil

Water content / %	Specific gravity	Liquid limit / %	Plastic limit / %	Grain-size distribution / %		
				Sand	Silt	Clay
50	2.70	48.3	30.1	0	71.1	28.9

The model pond was made of Plexiglas with a size of 600mm×600mm×400mm. A 1000 ml graduated cylinder was placed in the bottom of the tank to measure the drainage volume. The thickness of soil was 200mm and the distance between the cathode and anode was 200mm too. The electrode with a length of 250mm was arranged in the hexagonal pattern. The potential probes were embedded in the soil as shown in Figure 1. The model of power supply was ITECH-IT6863A and its maximum voltage was 72V.

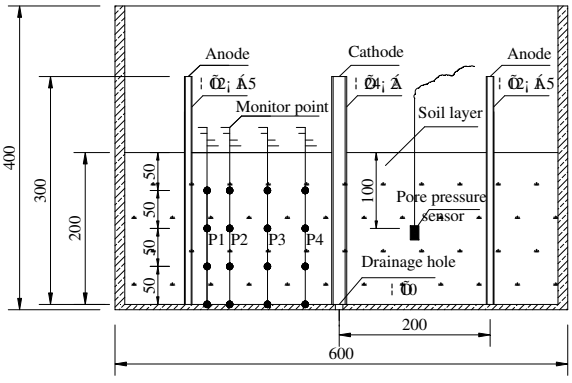

(a) Section view

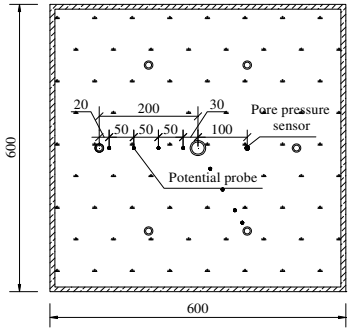

Unit: mm

(b) Vertical view

Figure 1 Schematic of the electro-osmotic model device

There were two kinds of electrodes used in the test, the iron electrode and the new type of EKG electrode. The size of the iron electrode which was used as anode and cathode was φ12×1.5mm and φ24×2mm respectively. On the surface of the cathode, there were dislocated circular holes with diameter of 5mm. The new type of EKG electrode was electrically conductive and its shape was shown in Figure 2. The electrode was surrounded by a membrane and it was electrically conductive either. The electrical resistivity of the EKG electrode and iron electrode was $1\times10^{-3}\Omega\cdot m$ and $1\times10^{-7}\Omega\cdot m$ respectively. The EKG electrode was composed of polyethylene, carbon black and graphite in the proportion of 20:7:2.

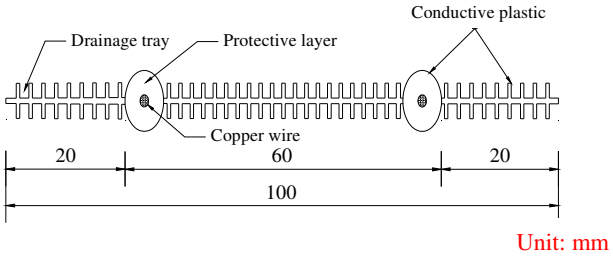

Figure 2 Schematic of the EKG electrode

2.2 Methods

To compare the electro-osmotic drainage effect between the EKG electrode and the iron electrode, three kinds of comparative tests were carried out, as shown in Table 2. The power supply was activated and its rotary knob was turned to the predetermined position. The drainage amount and electric potential distribution were measured every 2 hours and the current was measured every 4 hours. The test stopped when the water discharge was lower than 2ml per hour and the whole test lasted approximately 160 hours. At the end of each test, the water content at different positions was measured.

Table 2 Test programs

Test number	Voltage / V	Electrode material	Initial water content / V
T1	20V	Iron	49.9
T2	20V	EKG	50.0
T3	30V	Iron	50.1
T4	30V	EKG	49.8
T5	40V	Iron	50.2
T6	40V	EKG	49.9

3. RESULTS AND DISCUSSION

3.1 Drainage volumes and drainage rate

Figures 3 and 4 show the total drainage volume and the top surface drainage volume. The total drainage volume represented the total drainage ability of the material during the electro-osmosis process, with the assumption that water could be discharged as soon as it reached the cathode. Top surface drainage volume represented the top surface drainage ability of the material. Because water was always drained out from the top surface of the reclaimed soil foundation, it was also measured specially.

As shown in Figure 3, the total drainage volume increased dramatically in the first 75 hours, and increased gently in the following 100 hours. The total drainage volume of the new type EKG electrode was smaller than that of the iron electrode at the same voltage. It was primarily due to the conductivity of the iron electrode was better than the EKG electrode.

As shown in Figure 4, the drainage volume from the top surface of the soil increased with the applied voltage. Drainage volume of the EKG electrode was higher than that of the iron electrode at the same voltage. It was mainly due to that the EKG electrode was designed to be plate board shape, while the iron electrode could only be the cylinder or pipe shape considering stiffness and corrosion. The water could be discharged from the top of the soil more easily for the EKG electrode. In addition, the water was always discharged from the top surface of the reclaimed soil foundation and additional drainage channel needed to be arranged around the cathode of the iron electrode in the field trials. Considering from this aspect, the EKG electrode was superior to the iron electrode.

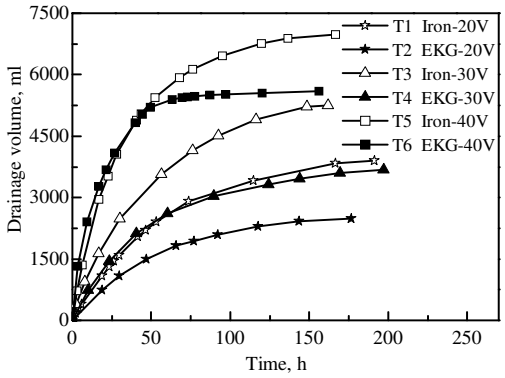

Figure 3 Variation of the total drainage volume with time

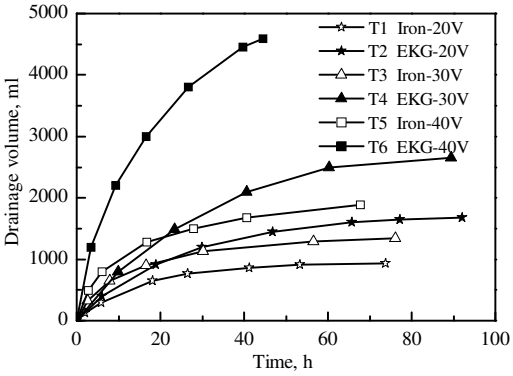

Figure 4 Variation of drainage volume from the top surface of soil with time

Figure 5 showed the variation of drainage rate from the top surface of the soil. The drainage rate declined dramatically for the T5 and T6 but declined gently from T1 to T4. It declined substantially in the first 75 hours but declined gently in the following 100 hours for the 6 groups of tests. It was uneconomical to continue the test after 75h. For instance, the drainage rate of T5 had declined from 260ml/h to 20ml/h and only a small portion of the water was drained in the following 125 h. Therefore, in field applications, the drainage rate should be monitored continually and further improve the drainage rate by changing the applied voltage or adding some buffer solutions (Rittirong et al. 2008).

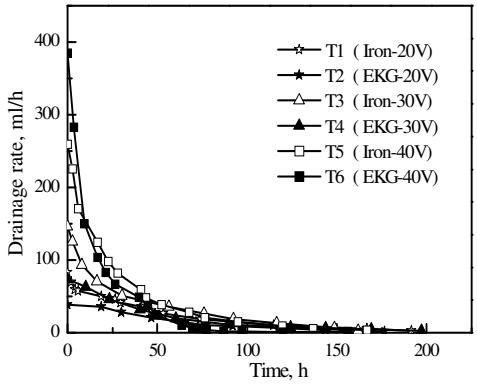

Figure 5 Variation of drainage velocity from the top surface of soil with time

3.2 Current and resistance

Figure 6 shows the variation of current with time. As shown in this figure, the current declined consistently after a brief rise (2h~3h). The entire process was continuous without any abrupt change. By comparing among T1, T3 and T5 or T2, T4 and T6, it can be seen that the higher the voltage, the greater the current change rate and the shorter the duration of the current upswing phase. After 150 hours, the current of T5 was lower than T1, for instance.

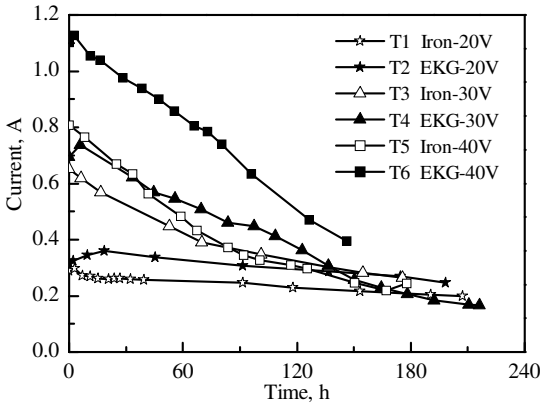

Figure 6 Variation of current with time

Figure 7 shows the variation of resistance with time. As shown in this figure, resistance increased gradually at 20V but increased dramatically at 40V for the EKG and iron electrode. Comparison among T2, T4 and T6 shows that the higher the voltage, the lower the resistance within 100 hours. However, resistance of T6 was higher than that of T2 and T4 after 100 hours. Three primary reasons may explain the above phenomenon: (1) the accumulation of gas around the electrode reduced the contact area between the electrode and the soil, (2) the acidification caused by water movement reduced the conductivity of soil and, (3) the cracks caused by the movement of water increased the soil resistance further.

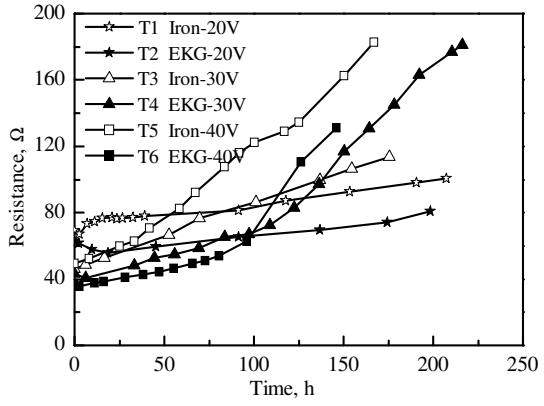

Figure 7 Variation of resistance with time

By combining the variation of current and the drainage amount, the energy consumption coefficient *C* could be acquired.

$$C = \frac{Q}{W} = \frac{\int_{t_1}^{t_2} UIdt}{\int_{t_1}^{t_2} qdt} \quad (1)$$

Where *C* is the energy consumption of unit drainage volume, *Q* is the total energy consumption, *W* is the total drainage amount in a particular period, *U* is the voltage applied in each test, *I* is the current and *q* is the drainage velocity.

The energy consumption coefficient *C* could be calculated by defining the time coefficient *t*. Provided that t_1=0*h*, t_2=30*h*, 75*h* or 120*h*, the energy consumption coefficient could be summarized as follows:

As shown in Table 3, the coefficient *C* would increase gradually with the increase of voltage. During the tests, a higher drainage rate could be obtained by improving the voltage and a higher *C* could be acquired. Because the energy consumption coefficient *C* at 120h had increased to double times of the coefficient on 30h. It was uneconomical to continue the test and methods need to be taken to reduce this coefficient, such as electrode conversion or intermittent electricity (Shang et al. 1997).

Table 3 Different energy dissipation coefficient

Tests / Time	T1	T2	T3	T4	T5	T6
30h	0.106	0.209	0.247	0.361	0.206	0.391
75h	0.134	0.261	0.272	0.483	0.293	0.516
120h	0.169	0.481	0.391	0.628	0.466	0.767

3.3 Potential distributions

There were 32 measuring probes embedded at different positions of the soil, as shown in Figure 1(a). The potential was monitored every 2 hours. Finally, the variation of potential on cross-section and longitudinal section was analyzed.

Figure 8 shows the variation of the potential of T5 and T6 at the depth of 100mm, with different distances (20mm, 50mm, 100mm and 150mm) from the anode. As shown in Figure 8(a), the potential drop on the Anode-P1 segment increased from the initial 7.5% to the final 20%, and kept stable around 65% on P4-Cathode segment. The effective voltage in P1-P4 section could account for 30% of the total voltage. As shown in Figure 8(b), the potential drop in Anode-P1 segment increased from the initial 17.5% to the final 25%, and kept declining from 52.5% to 37.5% in P4-Cathode segment. The effective voltage can only account for approximately one third of total voltage. However, because there was a better contact between the EKG electrode and the soil, the potential drop on electrode-soil surface of the EKG electrode was smaller than the iron electrode.

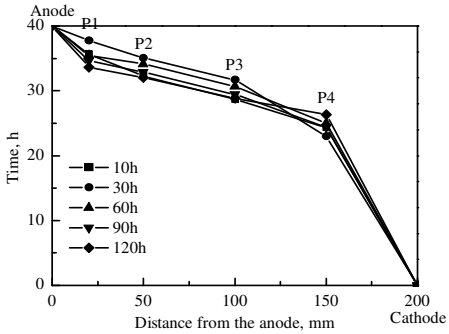

(a) The potential variation of T5

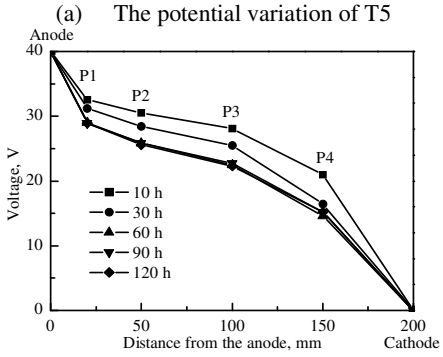

(b) The potential variation of T6

Figure 8 Variation of potential at 100mm depth of T5 and T6

Figures 9 and 10 show the distribution of potential on the longitudinal section (50mm, 100mm and 150mm in depth) of P1 and P3. The potential drop increased with time on the segment of Anode-P1 and Anode-P3, as shown in Figures 9 and 10.

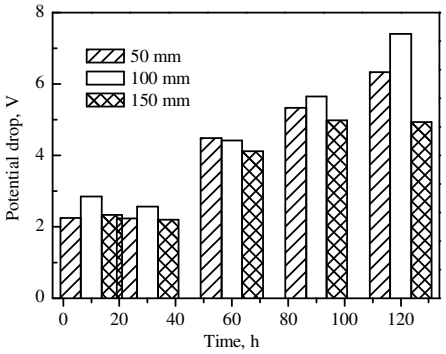

(a) Potential drop of T5 on Anode-P1 segment

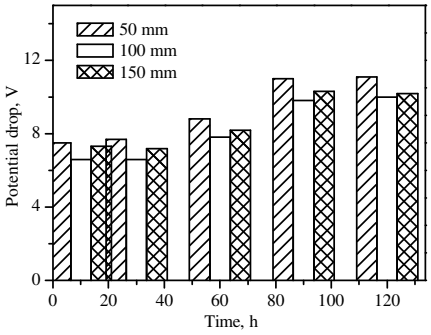

(b) Potential drop of T6 on Anode-P1 segment

Figure 9 Potential distribution on the longitudinal of P1 section

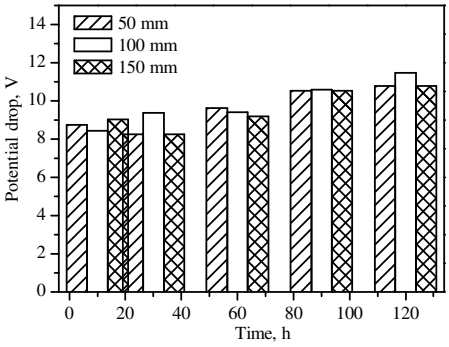

(a) Potential drop of T5 on Anode-P3 segment

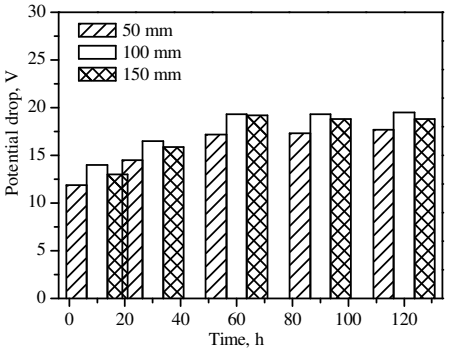

(b) Potential drop of T6 on Anode-P3 segment

Figure 10 Potential distribution on the longitudinal of P3 section

It was caused by the movement of water from the anode to cathode and the resistance would increase with the decline of water content. As shown in Figure 9, the potential drop of T5 at the depth of 100mm was larger than that in other depth. In contrast, it showed opposite rules in T6. It showed that the potential drop on the middle section of the electrode was larger than other positions. The intensity of the electrolytic reaction was higher at this point and the iron electrode was more susceptible to corrosion at this point.

3.4 Cracks development and electrode corrosion

The formation of cracks was induced by water movement, and it had a significant impact on the increase of resistance. In addition, electrode corrosion would increase the resistance and reduce the drainage rate. They were conjointly monitored.

Figure 11 shows the development of cracks at the end of the test. As shown in the figure, soil cracks in the iron electrode experiment were mainly formed in the anode and cathode connection while the cracks in the EKG electrode experiment mainly extended outward along the cathode plate wings. Part of the iron electrode had been out of contact with the soil around the cathode. Some iron rust had been integrated into the soil around the anode. Because the soil structure was destroyed under the scour of water, the drainage channel should be optimized so that the water around cathode could be discharged quickly.

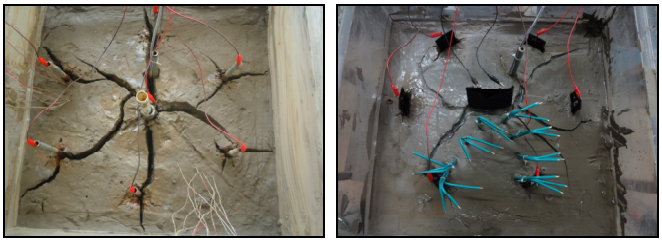

(a) Cracks development in T5 (b) Cracks development in T6

Figure 11 Cracks development in laboratory tests

Figure 12 shows the electrode corrosion after the test. It can be seen that the iron electrode eroded seriously while the EKG electrode kept intact. The durability of the EKG electrode was better than the iron electrode and its effect was more significant in field trials when the duration was longer than 30 days (Sun et al. 2015).

(a) The iron electrode (b) The EKG electrode

Figure 12 The corrosion of the electrode after the tests

According to the results of crack development and electrode corrosion, it could be concluded that the middle portion of the electrode should be treated with special attention. The cracks were induced by water movement which is normally from the anode to the cathode horizontally in theory. However, due to pore pressure dissipation around the cathode, it moved from anode to cathode in the upward sloping direction. As a result, most of the water above the middle section of the soil had been discharged, while the water below the middle section of the soil was retained in the soil. Because the electrolytic reaction occurred around the electrode and

the heat was released during the electro-osmosis process, the anode corroded easily at the junction of water, air and electrode. As a result, the middle portion of the iron electrode corroded easily and the EKG electrode was at the risk of aging.

3.5 Water content distributions

The homogeneity of soil in water content could be obtained by monitoring the moisture distribution after the tests. The soil samples were collected from 36 points and positions of the measuring points are shown in Figure 13.

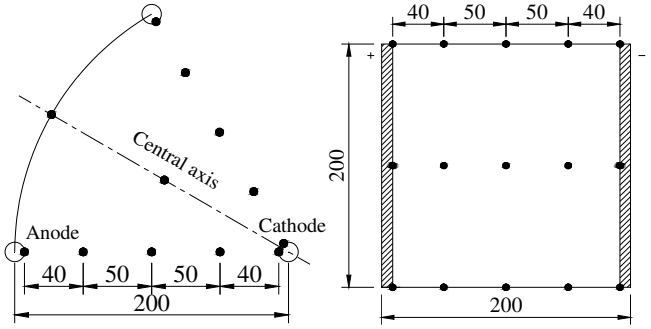

Figure 13 Layout of the measuring points

Figure 14 shows the water content distribution rule of the iron and EKG electrodes at 40V voltage after the tests. It showed different regularities of distribution from the anode to the cathode for these two kinds of electrodes. The water content in T5 increased gradually from the anode to the cathode while it increased gradually from the anode to the midpoint, and then declined steadily to the cathode in T6, without considering the decline of water content caused by exothermic reaction around the electrode. In addition, the water content increased in the vertical direction in T5 while declined gradually in T6. Moreover, the water content increased from the connection of anode-cathode to the central axis and the increase rate of iron electrode experiment was larger than the EKG electrode experiment. The homogeneity of the soil sample in the EKG electrode experiment was better than the iron electrode experiment.

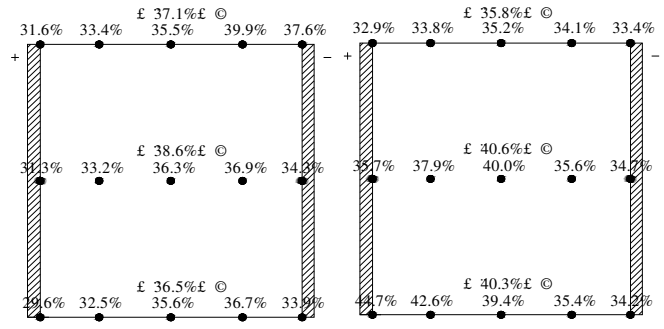

Figure14 The moisture content distribution

3. CONCLUSION

Comparing tests between a new type of EKG electrode and the iron electrode on different voltages were carried out. Major findings of the study are summarised below:

(1) The iron electrode eroded seriously while the EKG electrode kept intact. The top surface drainage capacity of the EKG electrode was better than that of the iron electrode. While the total drainage amount of the iron electrode was larger than the EKG electrode.

(2) The effective voltage can only account for one third of total voltage when the electrode was arranged in the hexagonal pattern and the potential loss on the electrode-soil surface of the EKG electrode was lower than that of the iron electrode.

(3) The cracks were developed by the water movement around the cathode and may reduce the treatment efficiency significantly. It could be inhibited by optimizing the drainage channel so that water could be discharged as soon as it reached the cathode.

(4) The anode eroded easily at the junction of water-air-electrode. As a result, the middle portion of the iron electrode corroded easily and the EKG electrode was at the risk of aging. It should be treated specially for the anode.

(5) The water content increased gradually from the anode to the cathode for the iron electrode. While it increased at first and then decreased from the anode to the cathode for the EKG electrode. It declined gradually along the depth for the iron electrode while increased gradually for the EKG electrode.

4. REFERENCES

Hu, Y. C., Wang, Z., Zhuang, Y. F., (2005). “Experimental studies on electro-osmotic consolidation of soft clay using EKG electrodes”. Chinese Journal of Geotechnical Engineering, 5, Issues 27, pp582-586.

Jones C J F P., (1996) “Briefing: Geosynthetic material with improved reinforcement capabilities”. Proceedings of the International Symposium on Earth Reinforcement, 2: pp865-883.

Jones C J F P., (2004) “Briefing: Electrokinetic geosynthetics: getting the most out of mud. Proceedings of the ICE-Civil Engineering, 3, Issues 157: 103.

Jones C J F P., John, L. B., Stephanie, G. (2011). “Electrokinetic geosynthetics in hydraulic applications”. Geotextiles and Geomembranes, Issues 29, pp381-390.

Rittirong A., Douglas R. S., Shang J. Q., Lee E. C., (2008). “Electrokinetic improvement of soft clay using electrical vertical drains”, Geosynthetics International, Volume 15, Issue 5, pp369-381.

Shang J Q., (1997) “Electro kinetic dewatering of a phosphate clay”. Journal of Hazardous Materials, 55, Issues 1-3, pp117-133.

Shang J Q. Electro kinetic dewatering of clay slurries as engineering soil covers. Canadian Geotechnical Journal, 1997b, 1, Issues 34, pp78-86.

Sun Z. H., Gao M. J., Yu X. J., (2015). Vacuum preloading combined with electro-osmotic dewatering of dredger fill using electric vertical drains [J]. Drying Technology. DOI:10.1080/07373937.2014.992529, In publish.

Zhuang, Y. F., Zou, W. L., Wang. Z., Tan, X. X., (2012). “A conductive plastic drain board China patent application”. CN 201220282864.